encit 2020

ABCM Associação Brasileira de Engenharia e Ciências Mecânicas

18th Brazilian Congress of Thermal Sciences and Engineering
November 16-20, 2020 (Online)

ENC-2020-0422
NUMERICAL INVESTIGATION OF CONDENSING FLOWS IN A SUPERSONIC SEPARATOR

Ulisses A. S. Costa
Luccas K. Kavabata
Ernani V. Volpe
Arthur S. Cato
Jairo C. Filho
Polytechnic School of the University of São Paulo - Av. Professor Mello Moraes, 2231 - Butantã, São Paulo - SP, 05508-030.
ulisses.costa@usp.br, luccas.kavabata@usp.br, ernvolpe@usp.br, arthur.cato@gmail.com, jairo.pcfilho@gmail.com

Marcelo T. Hayashi
Federal University of ABC, Av. dos Estados, 5001 - Santa Terezinha. Santo André - SP
mthayashi@gmail.com

Abstract. *The supersonic separation is a innovative technology, based on the adiabatic cooling of a swirling gas flow, and arise as promising new technique to remove water and heavy hydrocarbons from a natural gas mixture. However, the process of condensation in compressible flows, is still poorly understood. In this work, low-pressure condensing steam flows were investigated using the method of moments. The numerical results show that coupled nucleation models, such as the Hill's Method of Moments, can be used as a good approximation to analyze compressible flows in nozzle geometries. Also a comparison of the Static Pressure ratio along the nozzle, for different nucleation models was performed. The results were verified against experimental data of high-speed condensing steam measured at low pressure available in the literature.*

Keywords: *Homogeneous Condensation, Hill's Method of Moments, Supersonic nozzles, Nucleation.*

1. INTRODUCTION

One of the challenges pertinent to the development of natural gas reservoirs is to remove of contaminants from the mixture in order to make it economically attractive, through modern separation processes.

Nowadays there are different separation techniques such as the membrane, adsorption, absorption processes and so forth. However, this processes are not suitable if the gas mixture presents high concentrations of CO_2. In such cases a new technology, the supersonic separation, is being studied and is being developed aiming at removing most of the contaminants from natural gas, especially CO_2 due to environmental issues.

The Supersonic separation process is based on accelerating a swirling gas mixture to supersonic speed in a Laval nozzle where part of the flow's enthalpy energy is turned into kinetic energy. During the process the gas mixture is rapidly cooled and, as a result of the temperature drop, some of its components, e.g., CO_2, may condense. The swirl then centrifuges liquid phase towards the inner walls of the nozzle where it is removed through collectors.

This separation process is quite complex since it involves several phenomena such as condensation (and eventually re-evaporation) of the components of a gas mixture, compressible viscous flow, turbulence, and a swirling flow of a gas mixture. The main goal of the present paper is to investigate the condensation phenomena which is one of the main phenomena that occur in a supersonic separation.

The condensation models available in the literature split the phenomena into two: the nucleation of liquid droplets with critical size and the growth rate of these droplets. Nucleation can be defined as the kinetic processes that is involved in the beginning of a first-order phase transition, whereby a metastable phase becomes a more stable phase. The system may remain in the metastable state for a long time without transitioning to the most stable state, until it is destabilized by changing an external parameter such as temperature or pressure. Many researchers, interested in investigating the nucleation process, use convergent-divergent nozzles due to the facility in controlling the conditions of the experiment. As for the growth rate, it is related to the growth of the newly formed liquid droplets.

The condensation processes in supersonic flow was first analyzed by Oswatitsch (1942), and the effect of condensation on the flow field parameters was calculated. Hill (1966) simulated the condensation process of water vapor in a nozzle and found that the simulation results were in good agreement with the experimental data, when the surface tension was

assumed independent of droplet curvature. Moses and Stein (1978) obtained the precise data of condensation wave in a Laval nozzle, and the result has been widely used in validating mathematical models. J.B. Young (1992) were the first to perform 2D simulations for a condensing steam flow. Azzini and Pinni (2017) investigated non-equilibrium condensing flows through a quasi-1D Euler model, coupled with the method of moments, for the physical characterization of the dispersed phase.

The challenge of numerically reproducing the exact point where the condensation wave occurs mainly depends on the accuracy of the nucleation rate equation used. As a contribution to overcoming condensation challenges, the main objective of this series simulations was to investigate the numerical precision of the CFD open source code *Stanford University Unstructured* (SU2) to correctly capture the occurrence of a condensation wave, and to analyze the nucleation of liquid droplets through the moments of order zero to three. Thus, the physical understanding and accurate numerical modeling of the condensation process should be of great relevance to the design process.

2. LITERATURE REVIEW

2.1 Condensation phenomena

The first thermodynamic approach to the nucleation process is owed the American scientist Gibbs (1878), who demonstrated the dynamical theory of curved surfaces. Through his works it became clear that reversible work is required to form a new phase nucleus, and that it consists of a volumetric term and a superficial term.

$$\Delta G = -\frac{4}{3}\pi r^3 \rho_l R T_v \ln S + 4\pi r^2 \sigma \tag{1}$$

Where r is the droplet radius, R is the gas constant, T_v is the vapor temperature, σ is the surface tension,and S is the supersaturation ratio, which is given by

$$S = \frac{P_v}{P_S(T_v)} \tag{2}$$

where P_v is the vapor pressure and $P_S(T_v)$ is the saturated vapor pressure at temperature T_v.

For condensation to take place,it is necessary that the droplet radius r be larger than a certain value, which is commonly referred to as the critical radius (r_c).

On differentiating equation (1) with respect to the droplet radius r it is possible to obtain an expression for the critical radius.

$$r_c = \frac{2\sigma}{\rho_l R T_v \ln S} \tag{3}$$

Most condensation simulations are based on a nucleation rate and a droplet growth rate models. Some of the models used in the present work are presented briefly in the following subsections.

2.2 Nucleation rate

Classical Nucleation Theory The first theory on condensation phenomena is the Classical Nucleation Theory (CNT). It assumed that liquid droplets are all spherical and that the vapor phase and liquid phase have the same temperature. The nucleation rate for the CNT is given by:

$$J_{CNT} = q_c \frac{\rho_v^2}{\rho_l}\left(\frac{2\sigma}{\pi m^3}\right)^{1/2} \exp\left(-\frac{4\pi r_c^2 \sigma}{3kT_v}\right) \tag{4}$$

Where q_c is the condensation coefficient , ρ_v is the density of the vapor phase, ρ_l is the density of the liquid phase, m is the mass of a molecule, and k is the Boltzmann constant.

Although the CNT was able to predict the occurrence of condensation, it failed to predict it accurately. Therefore several corrections have been proposed to this theory.

Non-Isothermal correction One of the corrections proposed to the CNT is the non-isothermal correction, which drops the assumption that the vapor and liquid phases have the same temperature. The non-isothermal nucleation rate is given by:

$$J_{NonIso} = \left(\frac{1}{1+\phi}\right) q_c \frac{\rho_v^2}{\rho_l}\left(\frac{2\sigma}{\pi m^3}\right)^{1/2} \exp\left(-\frac{4\pi r_c^2 \sigma}{3kT_v}\right) \tag{5}$$

Where ϕ is given by:

$$\phi = q_c \frac{\rho_v R}{\alpha_r} \sqrt{\frac{RT_v}{2\pi}} \frac{H_e}{RT_v} \left(\frac{H_e}{RT_v} - \frac{1}{2} \right) \tag{6}$$

here, H_e is the specific enthalpy of evaporation and α_r is the surface heat transfer coefficient of a droplet whose radius is equal to the critical radius r_c.

Internally Consistent Classical Theory (ICCT) Another nucleation rate model is the one proposed by the Internally Consistent Classical Theory (ICCT). According to Lamanna (2000) it is given by

$$J_{ICCT} = 0.01 \frac{q_c}{S} \frac{\rho_v^2}{\rho_l} \left(\frac{2\sigma}{\pi m^3} \right)^{1/2} \exp\left(\frac{\sigma a_0}{kT_v} \right) \exp\left(- \frac{4\pi r_c^2 \sigma}{3kT_v} \right) \tag{7}$$

where S is the supersaturation rate and a_0 is given by

$$a_0 = (36\pi)^{1/3} \left(\frac{m}{\rho_l} \right)^{2/3} \tag{8}$$

where m is the mass of a molecule, and ρ_l is the liquid density.

Factor f correction Another correction is the factor f correction, which adds a factor f to the exponential term in equation (5). Thus, it leads to:

$$J_f = q_c \left(\frac{1}{1+\phi} \right) \frac{\rho_v^2}{\rho_l} \left(\frac{2\sigma}{\pi m^3} \right)^{1/2} \exp\left(- f \frac{4\pi r_c^2 \sigma}{3kT_v} \right) \tag{9}$$

2.3 Growth rate

Another aspect of condensation models is the growth rate. There are several models available but the one used in this work is Hill's growth rate model, which is appropriate to be used with the Method of moments.

2.3.1 Hill's model

The growth rate model that was proposed by Hill is given by

$$\left. \frac{dr}{dt} \right|_H = \frac{P_v}{\rho_l H_e \sqrt{2\pi R T_v}} \left(\frac{\gamma + 1}{\gamma} \right) C_p^v (T_s(P) - T_v) \tag{10}$$

Where C_p^v is the vapor phase specif heat at constant pressure, γ is the specific heat ratio, R is the gas constant, P_v is the vapor pressure, ρ_l is the liquid density, H_e is the specific enthalpy of evaporation, T_v is the vapor temperature, and $T_s(P)$ is the saturated vapor temperature at pressure P.

2.4 The Method of Moments

Most condensation models are based on modelling the nucleation rate and the growth rate. However, these models do not express the evolution of the liquid phase nor the distribution of droplet radius. One of the possibilities of doing so is by means of the so–called Method of Moments. It is described here by closely following the analysis by Put (2003).

Consider the General Dynamic Equation (GDE), which is given by

$$\frac{\partial f}{\partial t} + \frac{\partial}{\partial r} \left(f \frac{dr}{dt} \right) + \frac{\partial (f u_i)}{\partial x_i} = J \delta (r - r_c) \tag{11}$$

Where f is the radius distribution function, J is the nucleation rate, dr/dt is the droplet growth rate, and δ is the Dirac delta distribution. The radius distribution function is given by:

$$f(r, \vec{x}, t) \equiv \frac{\partial n(r, \vec{x}, t)}{\partial t} \tag{12}$$

Where $n(r, \vec{x}, t)$ is the droplet number density - which is a function of the droplet radius r, space ($\vec{x}$), and time (t).

On multiplying equation (11) by r^n, where n is an integer power, and after some algebraic manipulations, one has

$$\frac{\partial \mu_n}{\partial t} + \frac{\partial(\mu_n u_i)}{\partial x_i} = J r_c^n + n\frac{dr}{dt}\mu_{n-1} \tag{13}$$

Where μ_n is the moment of order n which is defined as

$$\mu_n \equiv \int_0^\infty r^n f dr \qquad (n = 0, 1, ...) \tag{14}$$

In the condensation models, a four moment equations are used — the zeroth, the first, the second, and the third order moments. From equation (13), one gets:

$$\frac{\partial \mu_0}{\partial t} + \frac{\partial(\mu_0 u_i)}{\partial x_i} = J \tag{15a}$$
$$\frac{\partial \mu_1}{\partial t} + \frac{\partial(\mu_1 u_i)}{\partial x_i} = J r_c + \mu_0\frac{dr}{dt} \tag{15b}$$
$$\frac{\partial \mu_2}{\partial t} + \frac{\partial(\mu_2 u_i)}{\partial x_i} = J r_c^2 + 2\mu_1\frac{dr}{dt} \tag{15c}$$
$$\frac{\partial \mu_3}{\partial t} + \frac{\partial(\mu_3 u_i)}{\partial x_i} = J r_c^3 + 3\mu_2\frac{dr}{dt} \tag{15d}$$

Sometimes the moment equations are not expressed in terms of the moments (μ_n), themselves, but rather in terms of of the so–called liquid moments (Q_n), instead. The latter are defined as

$$\mu_n \equiv \rho Q_n \tag{16}$$

where ρ is the mixture density. Furthermore, the third order moment is related to the wetness fraction y by

$$y = \frac{4}{3}\pi\rho_l\mu_3 \tag{17}$$

where ρ_l is the liquid density. Then, on substituting the liquid moments into equations (15a) through (15c) and by expressing the third order moment in terms of the wetness fraction y in equation (15d), one obtains

$$\frac{\partial(\rho Q_0)}{\partial t} + \frac{\partial(\rho Q_0 u_i)}{\partial x_i} = J \tag{18a}$$
$$\frac{\partial(\rho Q_1)}{\partial t} + \frac{\partial(\rho Q_1 u_i)}{\partial x_i} = J r_c + \rho Q_0\frac{dr}{dt} \tag{18b}$$
$$\frac{\partial(\rho Q_2)}{\partial t} + \frac{\partial(\rho Q_2 u_i)}{\partial x_i} = J r_c^2 + 2\rho Q_1\frac{dr}{dt} \tag{18c}$$
$$\frac{\partial(\rho y)}{\partial t} + \frac{\partial(\rho y u_i)}{\partial x_i} = \frac{4}{3}\pi\rho_l\left(J r_c^3 + 3\rho Q_2\frac{dr}{dt}\right) \tag{18d}$$

According to White and Hounslow (2000) the zeroth order moment is the total number of liquid droplets per unit mass of mixture. The first order moment is related to the average droplet radius, the second order moment is related to the total droplet surface area, and the third order moment is related to the wetness fraction.

The moment equations must be solved along with the conservation equations. For a two-dimensional Euler case, for instance, the final system of equations reads:

$$\frac{\partial \mathbf{U}}{\partial t} + \frac{\partial \mathbf{F}_x}{\partial x} + \frac{\partial \mathbf{F}_y}{\partial y} = \mathbf{S} \tag{19}$$

where the augmented state vector $\mathbf{U}$ and the augmented flux vectors $\mathbf{F}_i$ are given by:

$$\mathbf{U} = \begin{bmatrix} \rho_v \\ \rho_v u \\ \rho_v v \\ \rho E_{0,v} \\ \rho_m y \\ \rho_m Q_2 \\ \rho_m Q_1 \\ \rho_m Q_0 \end{bmatrix}; \mathbf{F}_x = \begin{bmatrix} \rho_v u \\ \rho_v u^2 + P \\ \rho_v uv \\ \rho_v H_{0,v} u \\ \rho_m y u \\ \rho_m Q_2 u \\ \rho_m Q_1 u \\ \rho_m Q_0 u \end{bmatrix}; \mathbf{F}_y = \begin{bmatrix} \rho_v v \\ \rho_v uv \\ \rho_v v^2 + P \\ \rho_v H_{0,v} v \\ \rho_m y v \\ \rho_m Q_2 v \\ \rho_m Q_1 v \\ \rho_m Q_0 v \end{bmatrix}; \mathbf{S} = \begin{bmatrix} S_m \\ S_m u \\ S_m v \\ S_m H_{0,l} \\ \frac{4}{3}\pi\rho_l(J r_c^3 + 3\rho_m Q_2 G) \\ J r_c^2 + 2\rho_m Q_1 G \\ J r_c + \rho_m Q_0 G \\ J \end{bmatrix}; \tag{20}$$

Here, $\rho E_{0,v}$ is the total energy of the vapor phase, $H_{0,v}$ is the total enthalpy of the vapor phase, $H_{0,l}$ is the total enthalpy of the liquid phase, G is the growth rate (dr/dt), ρ_m is the mixture density, and S_m is related to the mass exchange between the vapor and liquid phases and it is given by Azzini and Pinni (2017)

$$S_m = -3\rho_m \frac{y}{R}\frac{\partial R}{\partial t} \tag{21}$$

where R is the average droplet radius.

3. COMPUTATIONAL METHODS

A branch of the SU2 suite, an open-source CFD solver for performing Partial Differential Equation (PDE) integration, called *turbo_2phase*, which was developed by researchers from TU Delft Azzini and Pinni (2017), was used for the calculations of the two-phase flows. The numerical approach was based on a finite-volume method and the time discretization method used was the Euler implicit method. The Upwind difference schemes was used to compute the convective flux derivatives.

The mesh generation in 2D and 3D is a real challenge due to the complex characteristics and phenomena at various scales that a flow may have: boundary layers, shock waves and turbulence. Clearly to capture such phenomena, the researchers must choose a robust and reliable mesh generator. All meshes of this work were generated using the GMSH 4.5 software, a open source 3D finite element mesh generator and the built-in CAD engine.

4. NUMERICAL RESULTS AND DISCUSSION

4.1 Test Case A - Moses and Stein (2D Simulation)

The well–known Moses and Stein nozzle, which is a representative study of supersonic wet-steam flows, was used in this investigation. The Fig. 1 shows the results for a set of numerical experiments. The inlet pressure was kept at $P_0 = 39996,7$ Pa, while the inlet temperature was varied. The figure shows the normalized pressure trend along the axis and it focuses on the downstream region of the nozzle throat (x = 8.22 cm), where condensation shock occurs.

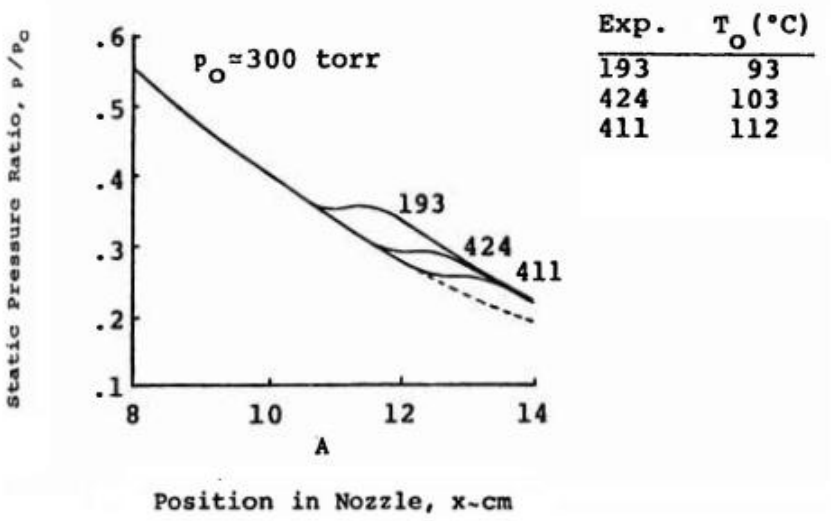

Figure 1: Comparison of pressure distribution for various flow conditions along the nozzle.
Source: Reproduced from Moses and Stein (1978)

In our simulations we have adopted the two-dimensional Euler equations, the Peng-Robinson-Streak-Vera (PRSV) equation of state (EoS) and a mesh of approximately 55 thousand elements. The set of boundary conditions for the simulations are summarized in Table 1.

Table 1: Flow parameters and boundaries conditions

Fluid	H_2O
Physical Problem	EULER
EoS	PRSV
Gas Constant	461.51(J/Kg*K)
Specific heat ratio	1.29
Critical Temperature	647.12 K
Critical Pressure	22060000 N/m^2
Critical density	322 Kg/m^3
Total pressure	0.25 bar
(Exp.424)- Total Temperature	369,15 K
Static outlet pressure	0.0625 bar
Spatial scheme	ROE - $1°order$

The moment of order zero which according to White and Hounslow (2000) is related to the total number of droplets per unit mass. It can be seen that condensation occurs at a specific location which is sometimes referred to as the condensation wave. The blue region in Fig. 2, represents the absence of water droplets, and it is clear that droplets only appears after the condensation wave.

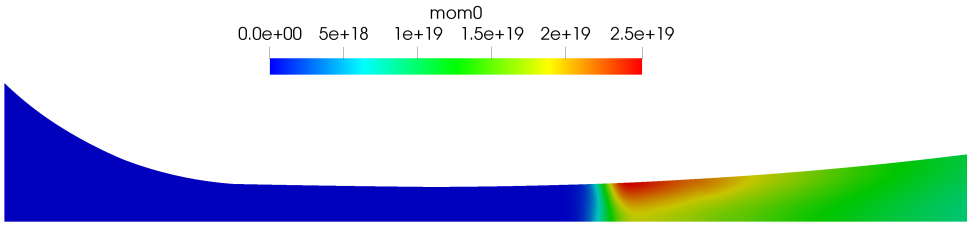

Figure 2: Moment of order zero obtained for case 424 of Moses and Stein (1978)

The Fig.3 presents the static pressure obtained for case 424. For simulating the low-pressure condensation flow in this nozzle, in addition to the Euler equations, the classical nucleation theory (J_{CNT}), eq. 5 was used. The Internally Consistent Classical Theory (J_{ICCT}), eq. 7, was adopted to determine the droplet formation. It is important to say that, initially, in the *turbo_2phase* only the classic nucleation rate (CNT) model had been implemented. The author of this work introduced two other models in the code: the ICCT model and the correction factor f.

The first simulations failed to predict correctly the position of the condensation wave, which is indicated by an increase in pressure due to phase change. One reason for this result is that the J_{CNT}, overestimates the nucleation rate of droplets with critical size. This discrepancy can be corrected if an appropriate constant term was introduced in the nucleation rate, as in Eq. (9).

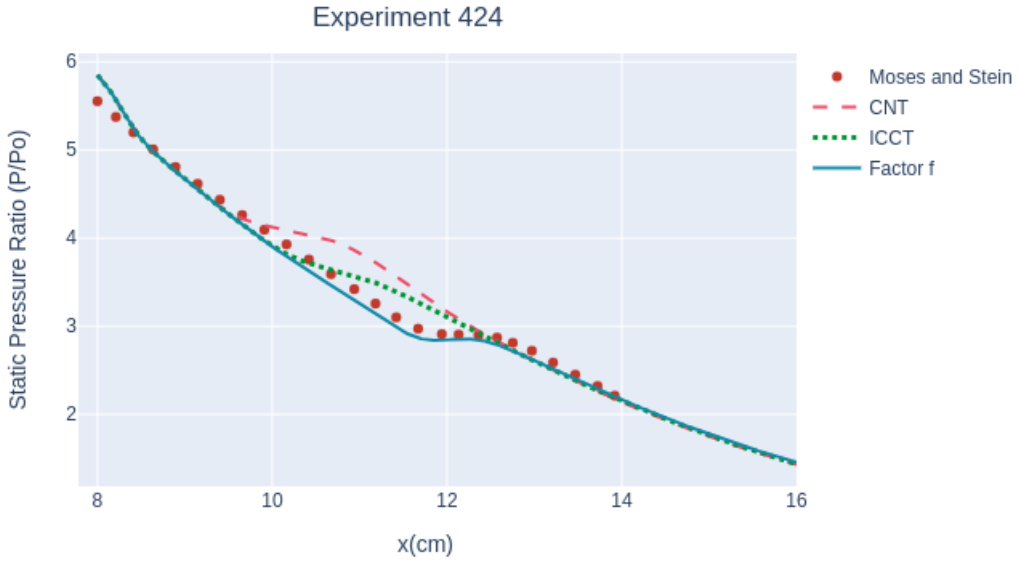

Figure 3: Comparison of the Static Pressure ratio along the nozzle,for different nucleation models.

The new simulation, represented by the blue line, shows that the correction factor ($f = 1.33$) captures a condensation wave very close to the points that represent the experiments of Moses and Stein. According to Grübel *et al.* (2018), there is no physical explanation for this factor yet, it is based entirely on experimental data.

The numerical results shown in Fig.4 correspond to the he zeroth order moment for different nucleation rate models, as they were found by the solver. As previously stated, this moment represents the total number of liquid droplets per unit mass of mixture and its result is intrinsically linked to the nucleation rate.

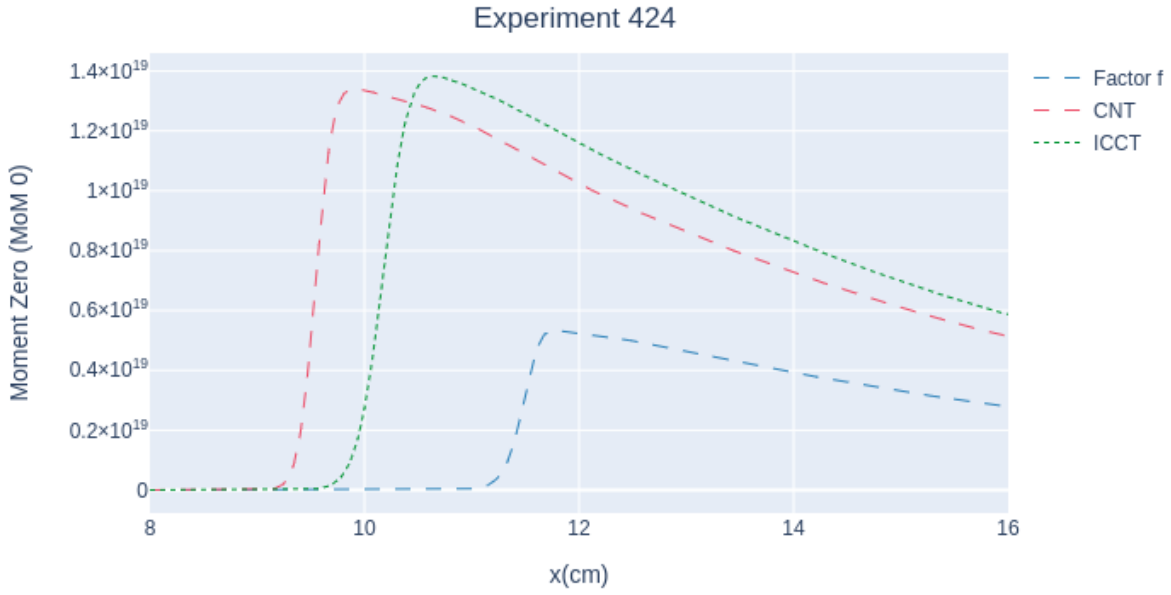

Figure 4: Comparison of the zeroth order moment for different nucleation models.

We can observe that for the CNT model, nucleation starts upstream at point x = 9.256 cm, while for the ICCT model, nucleation starts downstream at point x = 9.688 cm. The numerical values of both models for the zeroth order moment are not very different, however when comparing them with the model that was corrected by the introduction of the factor f, one clearly notices a significant decrease in the zeroth order moment value.

For a better understanding, the Table.2 shows the position difference between the numerical results obtained with the SU2 solver for case 424.

Table 2: Numerical results for zeroth order Moment.

Nucleation Rate Theory	Onset Condensation Position	MoM(0)'s Value
CNT	9.256 cm	$1.34 \, . \, 10^{19}$
ICCT	9.688 cm	$1.38 \, . \, 10^{19}$
Factor f	11.072 cm	$1.88 \, . \, 10^{18}$

4.2 Test Case B - Moses and Stein (3D Simulation)

A three-dimensional (3D) simulation of condensation phenomena was performed, in order to test the efficiency and accuracy of the code for three-dimensional meshes. The nozzle geometry is based on that of Moses and Stein's, the only difference being the fact that the Moses and Stein's nozzle used a rectangular cross-sectional area whereas a circular cross-sectional area has been used in the simulations. The 3D model of the nozzle which shows the moment of order zero along the length of the nozzle is shown in Fig. 5.

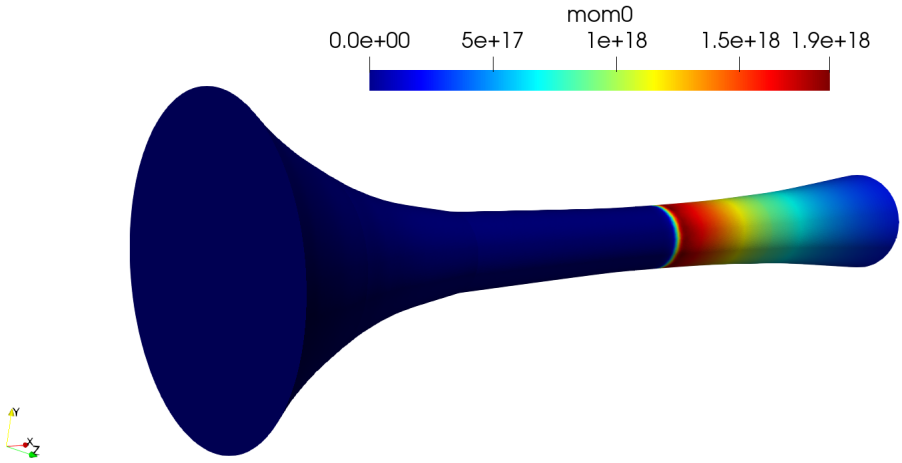

Figure 5: Three-dimensional model of Moses and Stein's nozzle which shows the moment of order zero.

It can be seen from Fig. 5 that initially there are no liquid droplets in the nozzle and that the first droplets begin to form in the divergent section of the nozzle, where the flow is supersonic and the temperature has dropped below the Wilson temperature.

It has already been pointed out that the occurrence of condensation leads to an increase in the flow static pressure. This is illustrated in figure 6 which shows a pressure over stagnation pressure (P/P_0) slice, with respect to the normal vector $(0, 0, 1)$. The flow static pressure is decreasing continuously when there is an increase in static pressure due to the occurrence of condensation. In figure 6 this can be seen as the slice color changes from a darker blue to a lighter blue.

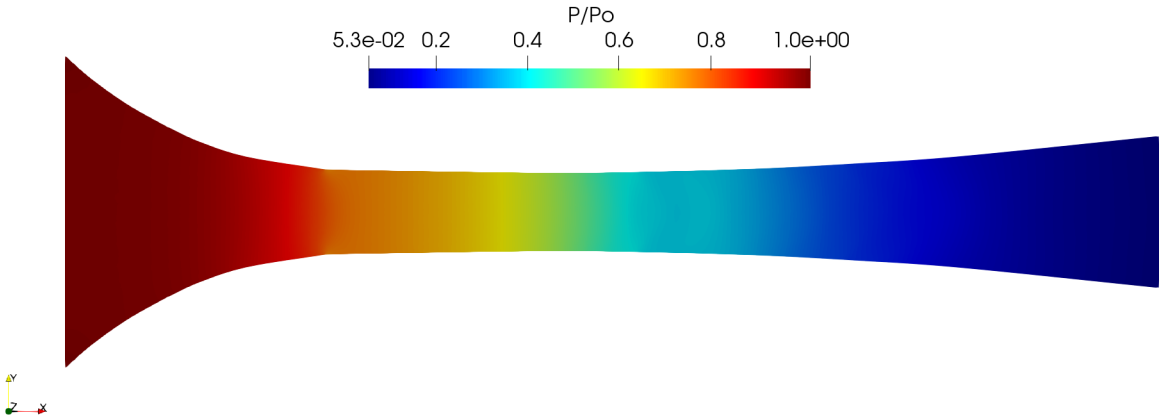

Figure 6: Pressure over stagnation pressure slice.

Figure 7 shows a slice, with respect to the normal vector $(0, 0, 1)$, of the moment of order three, which represents the wetness fraction .As was the case of figure 5, changes in the moment of order three can only be seen in the divergent section of the nozzle where condensation occurs.

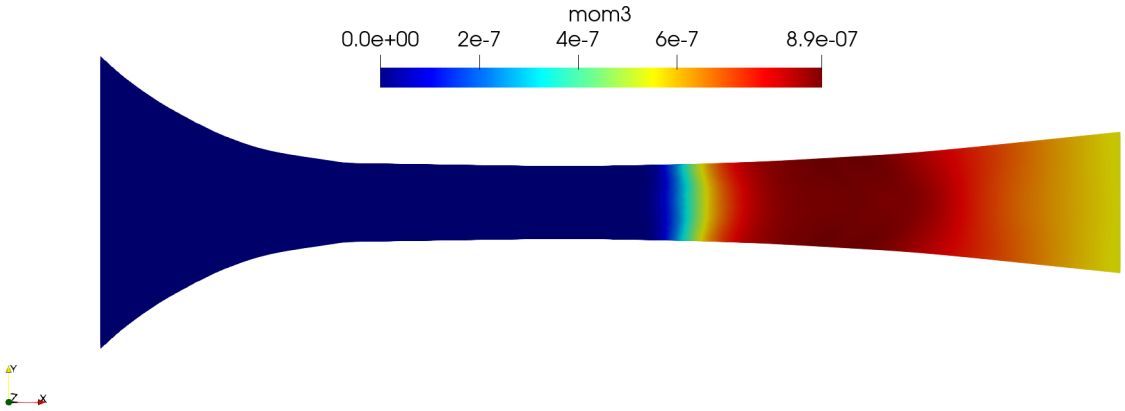

Figure 7: Moment of order three (wetness fraction) slice.

5. CONCLUSIONS

Numerical simulations have been performed in order to evaluate the different nucleation rate models under low pressure conditions. The fluid that is considered in this work is water vapor and it has been verified that the factor f correction produces the best results. For the curve P/P_0, where P_0 is the stagnation pressure, agrees quite well with Moses and Stein (1978) experimental data. The Hill's Method of Moments provides reasonably accurate predictions, especially when associated with a corrected nucleation rate. The numerical results show that the SU2 solver is capable of successfully simulating the condensation phenomenon for two-dimensional and three-dimensional problems.

6. ACKNOWLEDGEMENTS

The authors would like to thank the sponsorship of Shell and FAPESP through the "Research Centre for Gas Innovation - RCGI" (FAPESP Proc. 2014/50279-4), hosted by the University of Sao Paulo, and the strategic importance of the support

given by ANP (Brazil's National Oil, Natural Gas and Biofuels Agency) through the R&D levy regulation. The first author thanks CAPES and "Research Centre for Gas Innovation- RCGI" for the research scholarship. The authors would also like to thank the support of the National Council of Scientific and Technological Development (CNPq) and for the scholarship provided to the second author.

7. REFERENCES

Azzini and Pinni, 2017. "Numerical investigation of high pressure condensing flows in supersonic nozzles". *Journal of Physics: Conference Series*.

Gibbs, J.W., 1878. "On the equilibrium of heterogeneous substances". *Transactions of the Connecticut Academy of Arts and Sciences*, Vol. III.

Grübel, M., Starzmann, J., Schatz, M. and Vogt, D.M., 2018. "Modelling of condensing steam flows in laval nozzles with ansys cfx". *Proceedings of the Institution of Mechanical Engineers, Part A: Journal of Power and Energy*, Vol. 232, No. 5, pp. 571–575. doi:10.1177/0957650917730664. URL `https://doi.org/10.1177/0957650917730664`.

Hill, P.G., 1966. "Condensation of water vapour during supersonic expansion in nozzles". *J. Fluid Mech*, Vol. 25, pp. 593–620.

J.B. Young, A.W., 1992. "Homogeneous nucleation and shock wave interaction in condensing steam flows". *Acta Mechanica*.

Lamanna, G., 2000. *Numerical Modeling and Investigation of Unsteady Phenomena in Condensing Flows of Industrial Steam Turbines*. Ph.D. thesis, Eindhoven University of Technology.

Moses and Stein, 1978. "On the growth of steam droplets formed in a laval nozzle using both static pressure and light scattering measurements". *Trans. ASME J. Fluids*, Vol. 100.

Oswatitsch, K., 1942. "Kondensationserscheinungen in überschalldüsen". *J. Appl. Math*, Vol. 22, pp. 1–14.

Put, F., 2003. *Numerical Simulation of Condensation in Transonic Flows*. Ph.D. thesis, Universiteit Twente.

White, A.J. and Hounslow, M.J., 2000. "Modelling droplet size distributions in poly dispersed wet-steam flows". *International Journal of Heat and Mass Transfer*, Vol. 43, No. 11, pp. 1873 – 1884. ISSN 0017-9310. doi:https://doi.org/10.1016/S0017-9310(99)00273-2. URL `http://www.sciencedirect.com/science/article/pii/S0017931099002732`.

8. RESPONSIBILITY NOTICE

The authors are solely responsible for the printed material included in this paper.